J.K.A.U.: Mar. Sci., **Vol. 4**, pp. 93-114 (1413 A.H./1993 A.D.)

Mineralogy and Geochemistry of the Mesozoic-Tertiary Subsurface Sediments along Bardawil Lake, North Sinai, Egypt

A.M. GHEITH*, M.E. EL-SHERBINI and R. HASSAB ALLAH
**Faculty of Marine Science,*
King Abdulaziz University, Jeddah, Saudi Arabia, and
Faculty of Science, Geology Department,
Mansoura University, Egypt

ABSTRACT. An attempt is made in the present work to elucidate the mineralogy and geochemistry of the subsurface sediments in three deep wells drilled around lake Bardawil namely: Malha–1, El-Mazar–1 and Bardawil–1-1 in north Sinai.

X-ray diffraction analysis has been used to determine the bulk mineral content in 51 raw powdered samples of shale and limestone. It was found that kaolinite is dominant in Jurassic and Cretaceous deposits of El-Mazar well and in the Cretaceous deposits of Malha well. They have been formed during a period with warm climate and lowered sea level. While illite seems to be dominant in Jurassic deposits of Malha well indicating a tectonically unstable active area. The Oligocene, Miocene and Pliocene deposits of El-Mazar and Bardawil wells are characterized by dominance of montmorillonite and subordinate kaolinite, chlorite and illite revealing a humid climate with little changes. Source rocks and paleogeography are discussed.

X-ray fluorescence analysis has been carried out on the same raw samples of shale and limestone in order to determine the trace element content. The stratigraphic distribution of the trace element proved that Ba, Zr, Sr and Pb occur in higher concentrations in Jurassic and Cretaceous deposits of El-Mazar well, while Co, Cr, Cu, V, Pb and Ce are enriched in Pliocene and Pleistocene sediments. Seven geochemical stratigraphic units (chemozones) are distinguished in El-Mazar well.

Introduction

From latitude 30° to the north, alternating faulted domes, anticlines and synclines known as the Syrian arc, form a contrasting topography of low alluvial plains and high hill masses. Due to a series of down-to-basin faults, Neogene in age, the northern fringe of the Syrian Arc sinks seawards. It is hidden under the Quaternary coastal plain and the continental shelf deposits.

In northern Sinai, which represents the main objective of the present work, many deep wells have been drilled by IEOC. Among them three deep wells drilled by IEOC in 1986 around the areas of lake Bardawil (Fig.1) were given the names; Malha–1, El-Mazar–1 and Bardawil–1, penetrating rocks of Jurassic for Malha–1 and El-Mazar–1 and cretaceous for Bardawil–1.

The Jurassic sequence of Malha–1 is well developed and has a total thickness of 1120 m. The Jurassic sequence of El-Mazar–1 well is represented only by the late unit with thickness about 403 m. On the other hand, the Cretaceous overlies unconformably the Jurassic sequence of Malha–1 well and El-Mazar–1 well. The Early Cretaceous of Malha–1 well appears with thickness about 729 m. Meanwhile the Cretaceous of El-Mazar–1 well is represented only by the lower rock unit of thickness about 533 m. The Cretaceous of Bardawil–1 well is better developed. It appears more thick than in the other wells with thickness reaching 990 m.

As regards to the mechanism and timing of folding Carrey (1976) and Livermore and Smith (1985) assumed that during the late Cretaceous-Eocene, the eastern Mediterranean Sea had a compressional character as a result of subduction of the African-Arabian Plate beneath the Euro-Asiatic over thrusted margin. This produced faulting in the study area and thrusting of the Syrian Arc towards the south. During the Oligocene-Miocene normal fault systems were generated.

The composite lithologic logs provided by IEOC for the three wells in concern have been utilized for studying thickness and facies variations of the penetrated formations was constructed by Gheith *et al.* (1993) and represented in a correlation chart given in Fig. 2.

Material and Techniques

Fifty one samples of mud, marl and/or limestone have been chosen from the subsurface successions of the three studied wells; Malha–1, El-Mazar–1 and Bardawil–1.

Mineral content was determined by X-ray powder diffraction analysis using a Philips diffractometer with nickel-filtered Cu K_α radiation, at the Institute of Mineralogy, Karlsruhe University, West Germany.

For the identification of both non-clay and clay minerals the authors used the tables of key lines in X-ray powder diffraction patterns for minerals after Pei Yuan Chen (1977) and Chao (1969). In this investigation, oriented bulk samples were prepared so as to enhance the reflection of the clay minerals from the 001 crystal plane. The significant reflections used in identification of the different mineral species present in the samples are given in Table 1.

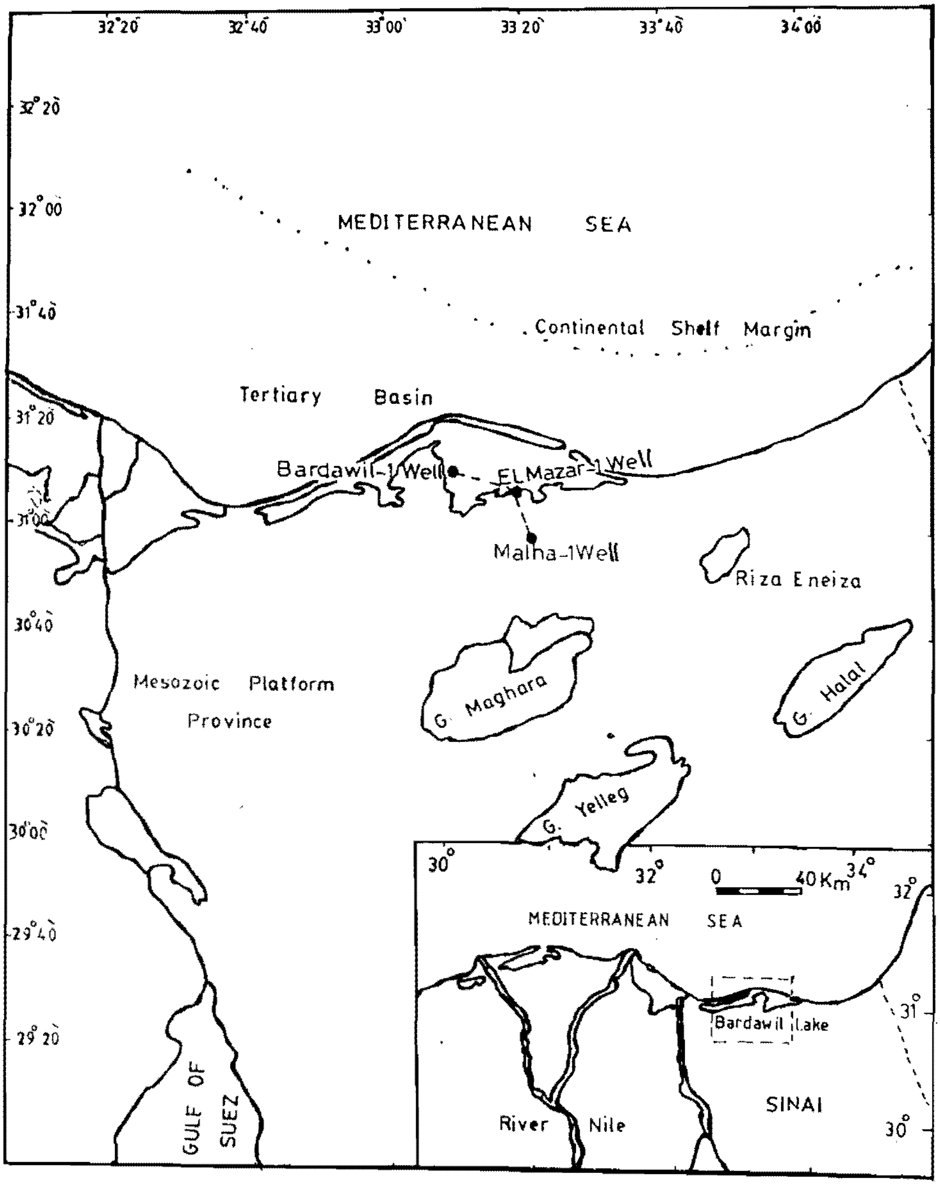

FIG. 1. Location map of North Sinai Wells (● studied wells) (Scale 1:500:000).

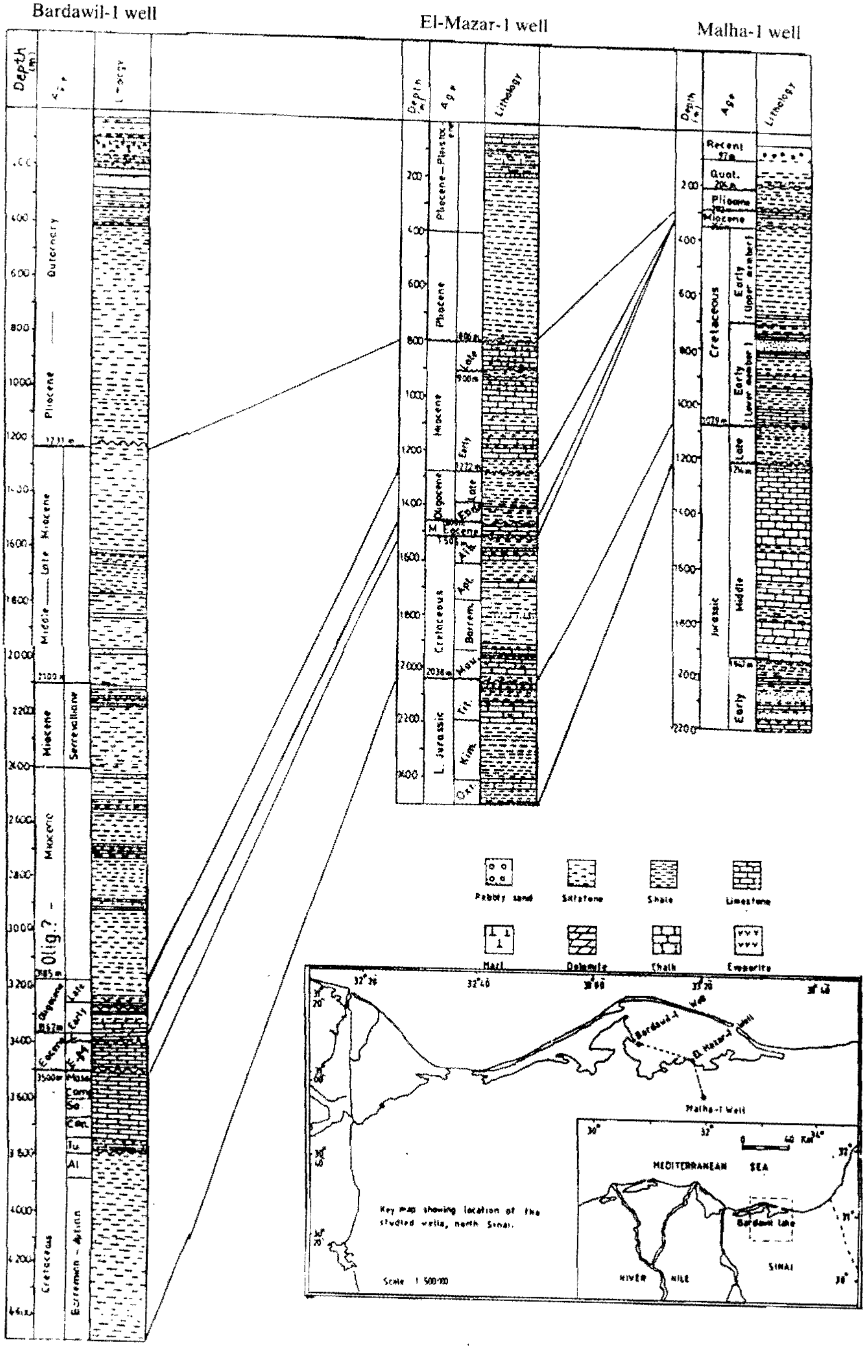

FIG. 2. Lithostratigraphic correlation chart showing the studied three sections in North Sinai.

TABLE 1. Significant reflections used in the identification of bulk minerals in the studied samples.

Bulk minerals	Identified minerals	2θ (001) Refl.	d(A°)	JCPDS (1974) §ASTM
Clay minerals	Montmorillonite	7.12	12.4	APX - 9
	Illite	8.75	10.1	2 - 462
	Kaolinite	24.87	3.58	§14 - 0164 ASTM
	Chlorite	25.15	3.54	§7 - 0171 ASTM
Detrital minerals	Quartz	26.86	3.34	5 - 490
	K-feldspar	27.49	3.27	§10 - 0479 ASTM
	Plagioclase feldspar	27.88	3.21	§9 - 0456 ASTM
Carbonate minerals	Calcite	39.37	3.04	5 - 586
	Dolomite	30.9	2.89	11 - 78
Sulphate	Gypsum	11.70	7.56	6 - 46
	Anhydrite	25.52	3.49	6 - 226
	Barite	25.89	3.44	5- 448
	Halite	31.7	2.84	5 - 628
	Pyrite	33.1	2.71	6 - 710

§Joint Committee on Powder Diffraction Standards.
American Society for Testing and Materials.

Geochemical analysis has been carried out on the whole rock powdered materials of 43 samples of shale and limestone composition. The common trace elements Ba, Sr, Zr, Cu, Zn, Ni, Co, Cr, V, Rb, Ga, Pb, Y, and Ce have been determined using the X-ray fluorescence technique. In addition, the relative percentage of organic matter in the rock powdered materials of El-Mazar–1 well has been determined by adding H_2O_2 until reaction ceased to remove organic matter.

Distribution and Significance of Bulk Minerals

The bulk mineral composition determined in percentage for fifty one samples chosen from the three wells; Malha–1, El-Mazar–1 and Bardawil–1 has been determined. The stratigraphical variation in mineralogical composition is illustrated in Fig. 3, 4 and 5.

Clay minerals, detrital constituents (quartz and feldspar), carbonate minerals, sulphate minerals and pyrite are the bulk constituents found in the subsurface sediments in north Sinai. The principal clay mineral components are montmorillonite, kaolinite, illite and chlorite in decreasing order of abundance.

The carbonate minerals are here represented by calcite which dominated over dolomite, while the sulphate minerals include scarce amounts of anhydrite, gypsum

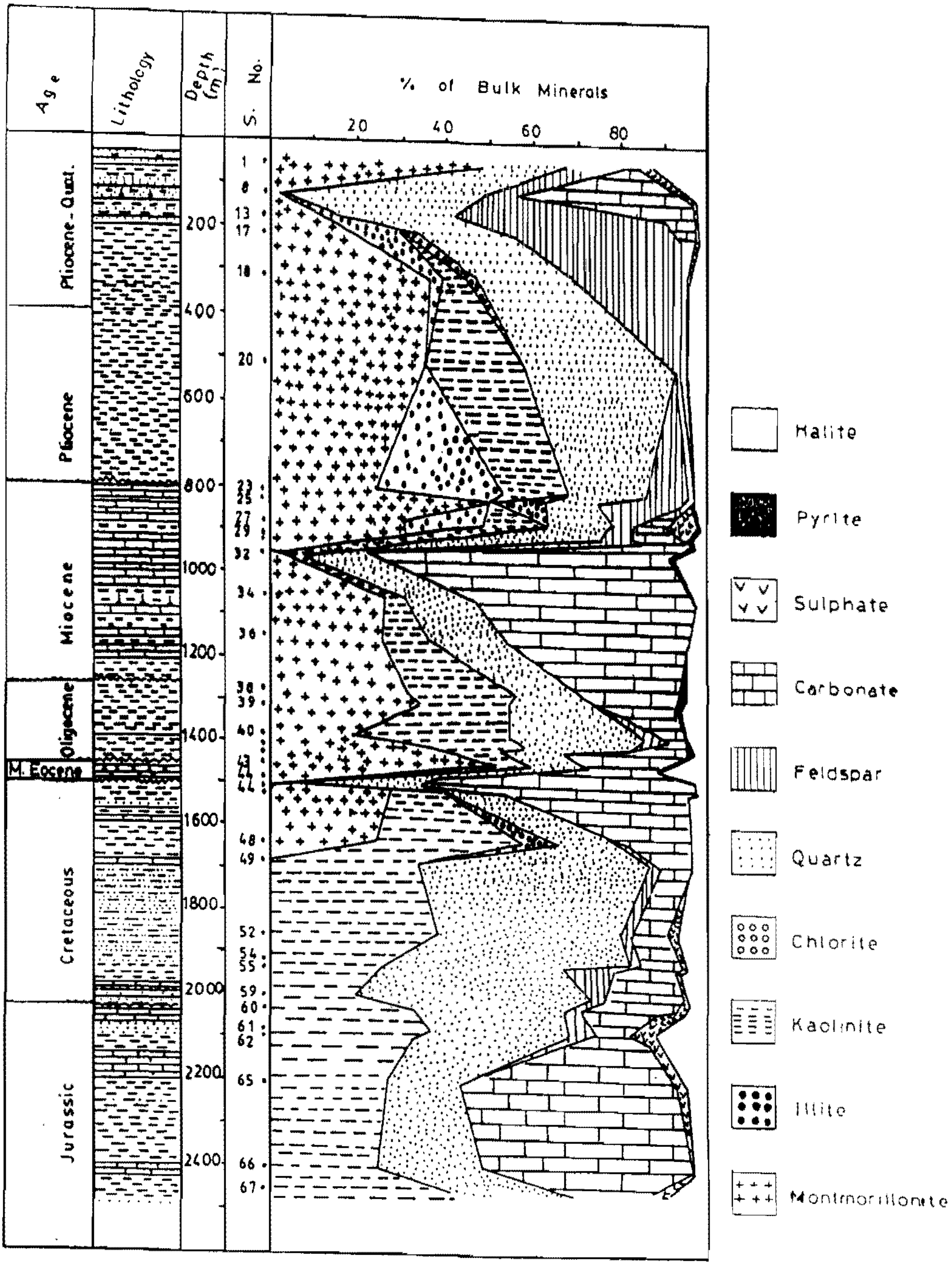

FIG. 3. Stratigraphical variation in mineralogical composition of the whole rock samples of El-Mazar–1 well (Data calculated as relative % from X-ray diffraction).

and barite. Generally, the distribution of these components show lateral and vertical variation.

The type of the source rocks, climate and the paleogeography are discussed.

1 – Stratigraphic Variation in Bulk Mineralogy of El-Mazar–1 Well

El-Mazar–1 well having an intermediate position, possibly represents a transitional stage between the other two wells; Malha–1 and Bardawil–1. A great number of samples were available and investigated from it. Thirty five samples of mudstone, marl and/or limestone have been analysed by X-ray diffraction. The stratigraphic variation of mineral constituents with depth is shown in Fig. 3.

In general, the clay mineralogy varied vertically with depth from Pre-Cretaceous to Quaternary. Montmorillonite is found to be the most abundant clay mineral constituents with minor content of kaolinite, illite and trace of chlorite. Kaolinite dominates in the Jurassic and Cretaceous sediments. The carbonate minerals represented by calcite which dominates over dolomite show cyclic variation with depth. Barite is very common among the mineral component of Jurassic and Cretaceous deposits. Several transgressive and regressive cycles can be traced through late Jurassic, late Cretaceous, Eocene and middle Miocene.

The Jurassic-Cretaceous boundary here, is marked by a distinct change of carbonate minerals which decrease upward with increase of quartz and feldspar constituents. The Miocene sediments are characterised by the association of clay minerals and carbonate minerals. The clay minerals are dominated by montmorillonite with subordinate kaolinite. At the end of the Miocene cycle it is clearly observed that there is a new association of minerals; evaporite, illite, chlorite and feldspar with considerable amount of montmorillonite.

However, the Pliocene sequence is very interesting due to the dominance of both clay minerals and the detrital constituents and feldspar while carbonate minerals are highly diminishing. Sediment supply was rather distinct during this period, where the continuous influx of detrital constituents took place through increased weathering of neighboring land mass. The clay minerals here are represented by montmorillonite, kaolinite, illite and chlorite in decreasing order of abundance. Feldspars show an irregular high content reaching up to 48%. The appearance of chlorite and illite indicates high latitude climatic conditions where mechanical weathering prevails. A cold-dry climate possibly alternated with humid climate at the source area during the Pliocene time. Afterwards, enrichment of calcite in the Pleistocene sediments, indicates seasonal humidity according to Biscaye (1965).

Tectonic events leading to uplifting and/or subsidence where erosion in up and down-stream areas producing rejuvenation of the relief, are also considered to be complementary factors in the differentiation of the clay mineral assemblages.

El-Gindy and Samuel (1978) mentioned that during the pre-Cenomanian times the greater part of Egypt remained a fairly stable uplifted and well-drained peneplained cratonic shelf under a warm climate. Such a continental environment encouraged extensive leaching of much weathered rocks so that kaolinite dominated the clay mineralogy of mud rocks of that period.

Since the Cenomanian, most of Egypt was transgressed by the Tethys. The echo of the laramide orogeny resulted in the strong tectonic folding of the "Syrian arc system" in its northern half. Marine sedimentation continued over a complex pattern of elongated subparallel narrow tectonic basins (Synclines and down faulted blocks) and later on over eroded structural ridges (Anticlinal Crests), domes and uplifted blocks thus montmorillonite dominated the clay minerals with subordinate kaolinite in marine post Cenomanian sediments. However, illite and chlorite are minor constituents of the majority of Phanerozoic mud rocks and marls in Egypt.

2 – Stratigraphic Variation in Bulk Mineralogy of Malha–1 Well

Nine samples have been analysed in this well and the data obtained is represented in a horizontal bars percentage (Fig. 4) which allows to record the following remarks :

1 – Four to five minerals are persistent throughout; clays, quartz, calcite and halite.
2 – Occurrence of montmorillonite is occasional; in the late Jurassic and Pliocene.
3 – Kaolinite and illite are almost consistent all through, but one increases on the expense of the other.
4 – Detrital quartz and feldspar increase towards the top almost on the expense of carbonates.
5 – The behavior of halite is peculiar. It has no stratigraphic trend.

A consideration difference between the Jurassic and Createaceous is documented here. Illite and calcite are the predominant components in the Jurassic, while kaolinite is the dominant mineral constituent during the cretaceous.

As a matter of fact the abrupt change in bulk mineralogy between Jurassic and Cretaceous indicates the effect of a late Jurassic movement of reasonable magnitude (Nevadian movement). The enrichment of illite in the Jurassic sediment of Malha–1 well bears close relation to river-borne sediment. Rivers are the principal carriers of fine-grained sediments from the continental source areas of high magnitude into the marine basins (Singer 1984). Furthermore, the strong tectonic activity leads to erosion in up and down stream areas and rejuvenation of the relief.

Otherwise, the abundance of kaolinite constituent in the Cretaceous sediments indicates a relatively warm climate acting on a terrestrial source with a peneplain topography (aggressive climate, Singer 1984).

It is concluded that tectonic events such as uplift and subsidence become a major importance in the Paleoclimate evaluation of clay minerals encountered in the subsurface sediments of Malha–1 well. Arid climate prevailed during the Cretaceous periods and humid with some scale aridity distinguishes the Jurassic. While the

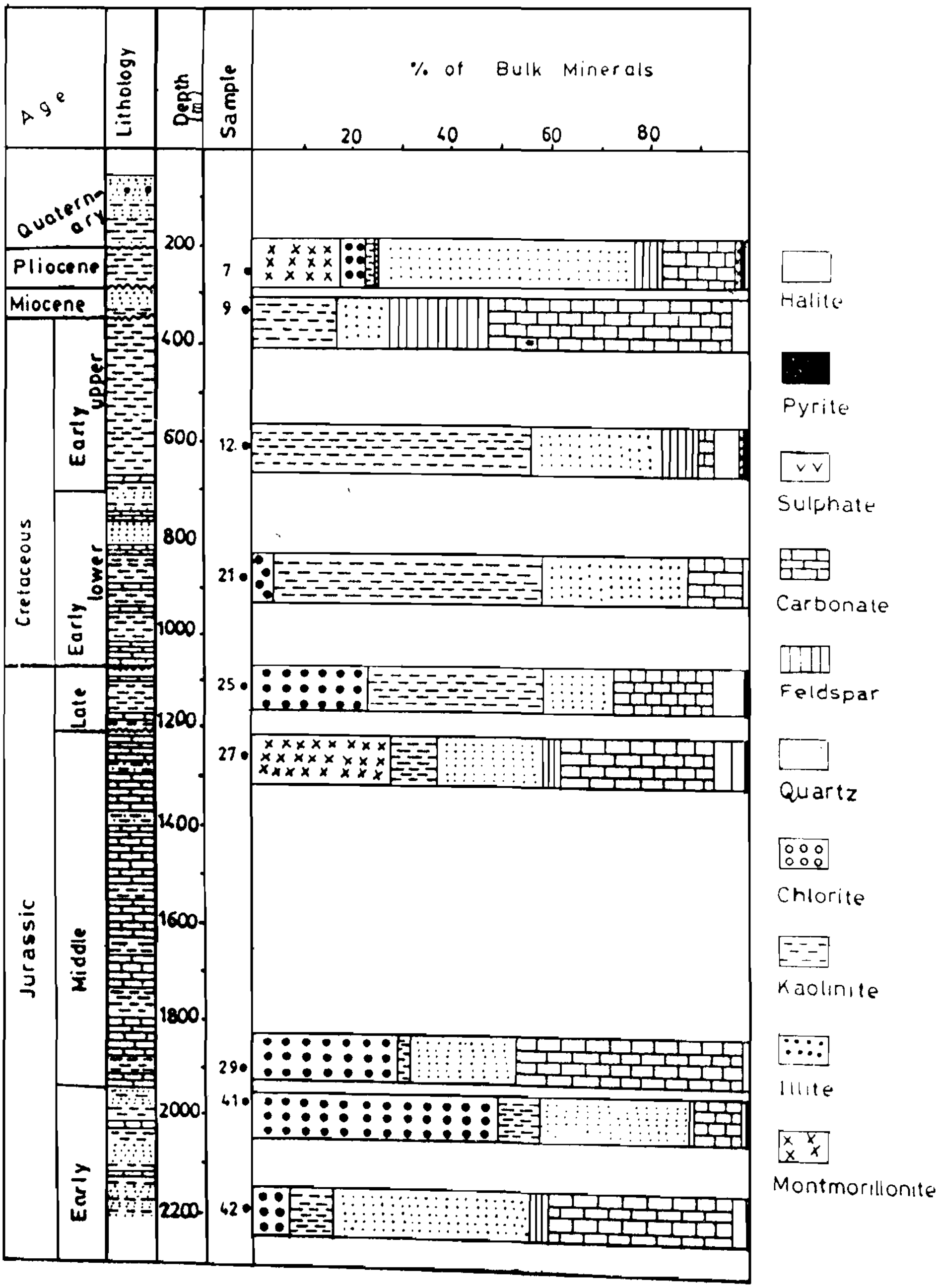

FIG. 4. Stratigraphic variation in mineralogical composition as bar diagrams of the whole rock samples of Malha-1 well (Data calculated as relative % from X-ray diffraction).

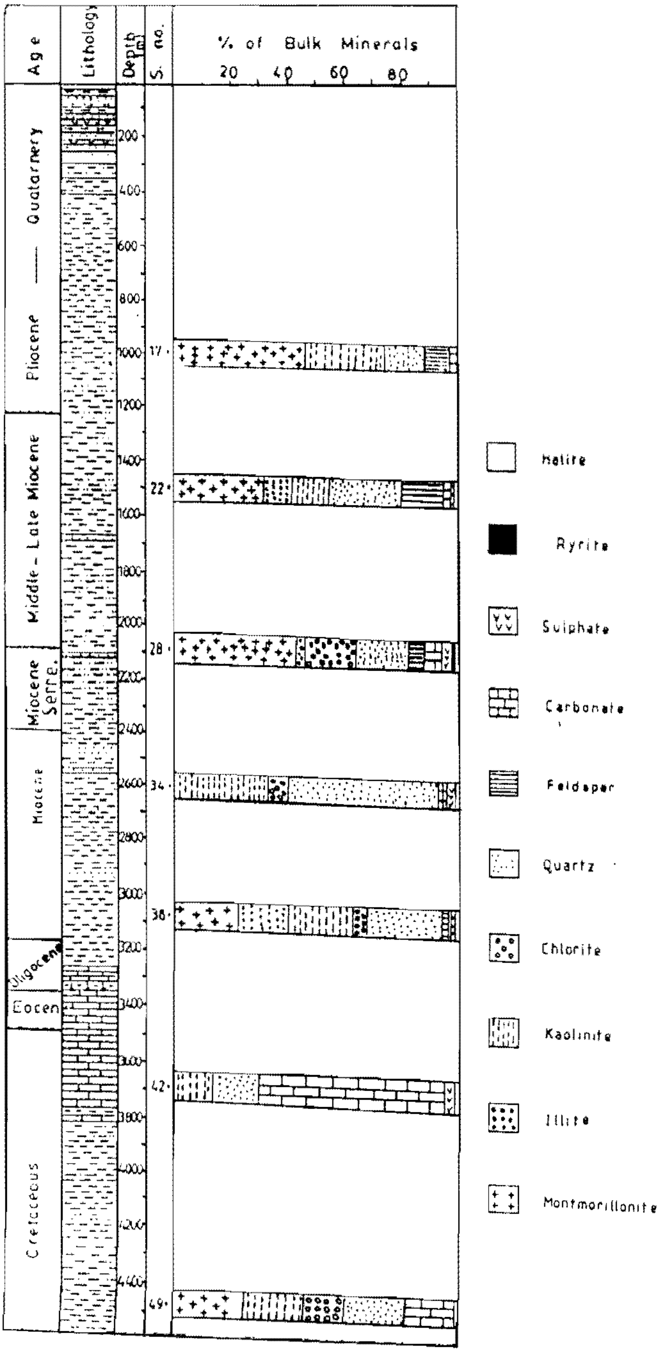

FIG. 5. Stratigraphical variation in mineralogical composition as bar diagrams of the whole rock samples of Bardawil–1 well (Data calculated as relative % from X-ray diffraction).

Miocene and Pliocene are characterized by numerous and strong changes between humid and arid periods (Chamely and Diester-Haass 1979).

3 – Stratigraphic Variation in Bulk Mineralogy of Bardawil–1 Well

Seven samples only have been anlaysed from Bardawil–1 well, (Fig. 5). As far as the data permits the following general observations are recorded :

1 It is found that montmorillonite is the dominant clay mineral component in the younger sediments (Miocene, Pliocene and Quaternary), while it become minor in the older sediments (Cretaceous).

2 – Carbonate exhibits an opposite trend of variation to montmorillonite and is enriched only in the Cretaceous sediments.

3 – Feldspar exhibits a similar behavior to montmorillonite; it is more abundant in the younger deposits.

4 – Kaolinite variation is erratic.

5 – Sulphate minerals are associated with the bulk mineral assemblage of Miocene sequence indicating an intertidal and supratidal environment where salinity increases due to a high rate of evaporation.

Trace Element Geochemistry

An attempt has been made herein to study the geochemical features regarding both abundance and vertical distribution of the trace elements in the bulk samples of the three studied wells; El-Mazar–1, Malha–1, Bardawil–1. The effect of organic matter on the concentration of trace elements and the potential of rocks for hydrocarbon generation are also discussed.

The results of these anlayses of elements have been calculated and given in Tables 3, 4 and 5. The trace element detected are Ba, Sr, Zr, Zn, Cu, Rb, Ga, Y, Pb, Co, Ni, Cr, Nb, and Ce. The stratigraphic distribution curves of these elements in the studied wells are shown in Fig. 6 and 8. Furthermore, the relative percentage of organic matter in the rock powdered materials of El-Mazar–1 well is presented in the variation curve shown in Fig. 8.

Trace elements can be used as indicator of environment and type of source rocks (Degens *et al.*, 1958; Hirst, 1962). Most minor elements enter the basin of deposition mainly structurally combined within the lattices of various clay minerals (Hirst 1962). Other processes possibly contributing to this concentration are association with organic carbon and association with the limonitic concretions.

These control mechanisms for concentration of trace elements, after Krauskopf (1956), are precipitation of sulphide within bottom sediments, adsorption and biological processes. Adsorption, according to Krauskopf, involves materials for which trace elements have affinity. These include clays, organic carbon and hydroxides.

Distribution and Significance of Trace Elements

A greater number of samples was available from El-Mazar–1 well providing a bet-

TABLE 2. Trace element contents in the bulk samples of Mesozoic-Cenozoic Subsurface sediments in Northern Sinai, Egypt. N.b. (Concentration in ppm)

S. No.	Depth (a)	Age		Lithology	Ba	Sr	V	Zr	Zn	Cu	Rb	Ga	Y	Pb	Co	Ni	Cr	Nb	Ce
	a – El-Mazar-1 well																		
1	41–50	Plio.?		Shale	297	312	102	303	396	729	56	18	42	47	21	59	105	37	82
17	200–210	Pleistocene		Shale	133	266	102	416	350	645	44	17	40	42	20	52	108	32	126
18	300–310	Pliocene		Shale	116	212	111	334	306	548	58	18	42	32	24	62	115	35	108
20	500–510			Shale	98	210	106	326	158	186	56	19	39	28	119	58	101	35	144
23	800–803			Shale	94	180	138	307	162	190	58	20	38	22	16	63	120	32	129
25	818–821	Lower Miocene		Shale	76	184	143	321	141	136	56	20	38	23	16	62	113	31	131
27	869–872			Calcereous shale	53	234	123	280	162	178	50	17	38	22	19	59	93	30	118
29	905–908	Middle Miocene		Shale	91	498	111	289	144	189	43	17	37	19	21	54	93	29	95
30	914–917			Shale	50	582	109	280	155	211	38	16	35	18	22	51	91	28	94
32	947–950	Early Miocene		Calcereous shale	31	887	84	220	113	114	33	14	38	18	22	43	68	23	115
34	1049–1058			Calcereous shale	30	787	67	152	123	159	20	12	28	15	19	34	54	13	48
36	1148–1151			Shale	81	770	81	181	125	148	30	12	31	12	19	42	74	18	48
38	1272–1277			Shale	55	617	82	240	107	48	32	14	33	16	19	43	70	27	111
39	1301–1304	Late Oligocene		Shale	105	368	147	347	129	55	33	18	41	23	20	56	103	45	147
40	1358–1388			Shale	191	290	203	433	155	85	29	22	46	20	24	61	117	60	170
41	1400–1403	Early Oligocene		Shale	199	461	154	335	135	56	32	19	43	18	21	52	101	45	157
42	1418–1420			Calcereous shale	244	611	115	225	140	91	34	15	37	21	20	44	99	31	103
43	1148–1451			Calcereous shale	252	567	122	214	128	69	39	18	35	19	17	36	88	29	89
44[£]	1478–1481	Middle Eocene		Calcereous shale	136	916	67	75	83	74	6	9	24	9	21	24	40	9	36
44	1499–1502			Limestone	139	902	66	45	72	78	2	8	21	9	24	23	33	4	3
45	1508–1511	Cretaceous	Alp.	Shaly Limestone	149	630	88	111	114	140	16	12	24	17	23	32	48	11	56
48	1631–1635		Apt.	Shale	745	394	76	244	118	121	49	16	31	78	18	32	51	30	91
49	1679–1682			Shale	554	279	83	385	127	110	40	18	36	53	19	38	68	35	176
52	1850–1853		Bar.	Sandy shale	3126	426	66	368	121	138	45	12	36	48	18	25	49	32	131
54	1919–1922			Sandy shale	2693	372	65	390	148	194	40	12	35	48	19	27	53	34	128
55	1934–1937		Hau.	Sandy shale	1868	391	65	316	301	535	34	13	33	49	19	32	56	30	124
60	2033–2036			Sandy shale	4356	649	61	439	152	231	14	9	39	40	18	17	39	36	86
61	2081–2084	Jurassic	Tito.	Sandy shale	5028	962	64	457	65	4	17	7	40	37	19	11	30	35	87
64	2098–2102			Sandy shale	4977	756	64	383	157	193	9	8	35	48	19	15	42	33	94
65	2166–2170		Kim.	Sandy shale	4747	864	64	191	129	173	2	7	26	26	19	13	39	14	40
66	2399–2402			Calcereous shale	2029	620	51	210	67	18	0	10	29	15	20	21	32	25	82
67	2450–2453		Oxf.	Shale	3139	676	63	401	60	7	10	9	42	24	19	17	35	47	99

b – Malha–1 well

7	250–260	Pliocene		Shale	63	329	39	299	121	227	27	11	30	22	20	27	52	16	60
8	92–300	Miocene		Sandy shale	42	289	68	400	130	152	31	15	32	103	19	34	68	33	131
12	501–504	Upper Cretac.		Shale	1757	322	96	555	163	148	17	18	50	34	14	41	100	70	210
25	1501–1104	Jurassic	Lat.	Shale	1356	560	74	314	196	321	29	15	40	30	16	39	77	42	128
27	1299–1302		Mid.	Calcereous shale	351	750	90	204	240	417	32	15	32	21	18	47	86	23	49
29	1901–1904			Shaly limestone	1256	354	46	98	780	1524	9	5	18	206	22	18	47	2	55
41	1962–1965		Ear.	Calcereous shale	929	323	91	479	661	1141	42	20	34	259	19	48	94	49	175
42	2180–2183			Calc. sandy shale	1308	309	42	255	850	944	22	10	26	89	29	34	46	17	83

c – Bardawil–1 well

17	980–1000	Pliocene	Shale	619	334	65	564	346	570	17	22	52	57	17	51	104	77	290
28	2085–2090	Miocene	Shale	10859	1043	110	397	89	78	52	9	46	26	18	22	46	33	25
34	2580–2609		Shale	8563	654	136	557	162	192	25	13	61	34	18	32	74	70	116
42	3680–3690	Cretaceous	Limestone	7783	1619	61	31	34	19	12	3	17	25	21	4	4	20	116

44£ : Add. sample.

TABLE 3. Correlation coefficient of elements for El-Mazar sediments.

	Ba	Sr	V	Zr	Zn	Cu	Rb	Ga	Y	Pb	Co	Ni	Cr	Nb	Ce	% Org. m.	% Clay m	% Carb. m
% Detrital m.	0.125	– 0.046	0.562	0.502	0.239	0.166	0.573	0.615	0.289	– 0.620	0.234	0.759	0.706	– 0.083	0.237	0.466	– 0.286	– 0.033
% Carbonate m	– 0.169	0.749	0.036	– 0.567	0.378	0.407	0.333	0.181	0.241	0.236	0.017	0.133	0.178	0.284	0.398	– 0.170	0.551	
% Clay m	– 0.027	– 0.728	– 0.457	– 0.789	– 0.437	– 0.348	– 0.632	– 0.640	– 0.737	– 0.411	– 0.123	– 0.358	– 0.567	– 0.747	– 0.632	– 0.643		
% Organic m	– 0.278	0.281	0.651	0.342	0.127	– 0.055	0.607	0.705	0.362	0.170	0.139	0.580	0.625	0.551	0.506			
Ce	– 0.169	– 0.667	0.560	0.725	0.222	0.052	0.580	0.683	0.763	0.319	0.174	0.509	0.558	0.806				
Nb	– 0.192	– 0.316	0.298	0.848	0.231	0.067	0.077	0.522	0.910	0.317	0.072	0.352	0.466					
Cr	– 0.650	– 0.742	0.841	0.732	0.506	0.341	0.607	0.932	0.617	– 0.097	0.249	0.939						
Ni	– 0.780	– 0.701	0.809	0.115	0.477	0.330	0.781	0.917	0.510	– 0.169	0.174							
Co	– 0.153	– 0.192	0.065	0.040	0.030	0.019	0.211	0.200	0.101	– 0.037								
Pb	0.387	– 0.352	– 0.251	0.498	0.390	0.387	0.042	– 0.042	0.054									
Y	– 0.913	– 0.551	0.581	0.824	0.429	0.227	0.537	0.572										
Ga	– 0.678	– 0.819	– 0.303	0.183	0.434	0.234	0.180											
Rb	– 0.487	0.816	0.449	0.324	0.334	0.423												
Cu	– 0.019	0.422	0.518	0.208	0.917													
Zn	– 0.136	– 0.544	0.078	0.285														
Zr	0.350	– 0.465	0.226															
V	– 0.545	– 0.573																
Sr	0.382																	

TABLE 4. Correlation coefficient of elements for Malha sediments.

	Ba	Sr	V	Zr	Zn	Cu	Rb	Ga	Y	Pb	Co	Ni	Cr	Nb	Ce	% Clay. m.	% Carb. m.
% Detrital m.	-0.568	-0.263	-0.470	0.127	-0.030	-0.195	0.038	-0.108	-0.098	-0.084	0.374	-0.201	-0.394	-0.156	-0.143	-0.486	-0.202
% Carbonate m.	-0.331	0.065	-0.509	-0.657	0.551	0.279	-0.239	-0.603	-0.719	0.151	0.428	-0.453	-0.602	-0.700	-0.597	-0.673	
% Clay m.	0.528	-0.204	0.727	-0.165	-0.040	0.209	0.613	0.549	0.137	0.084	-0.424	-0.709	0.778	0.708	0.617		
Ce	0.450	-0.203	0.656	0.926	-0.193	-0.250	0.219	0.763	0.785	0.151	-0.613	0.501	0.627	0.939			
Nb	0.386	-0.081	0.796	0.903	-0.402	0.472	0.677	0.426	0.937	-0.113	-0.679	0.677	0.866				
Cr	0.202	-0.247	0.980	0.711	0.399	-0.639	0.455	0.902	0.805	-0.069	-0.771	0.836					
Ni	0.043	0.422	0.529	0.567	0.201	-0.331	0.725	0.892	0.630	-0.107	-0.407						
Co	-0.034	-0.306	-0.717	-0.665	0.774	0.549	-0.190	-0.611	-0.745	0.268							
Pb	0.123	0.399	0.001	-0.014	0.700	0.814	0.099	0.047	0.442								
Y	0.313	0.413	0.723	0.816	-0.615	-0.684	-0.229	0.792									
Ga	0.012	0.114	0.852	0.844	-0.421	-0.547	0.712										
Rb	-0.477	0.221	0.432	0.244	-0.233	-0.241											
Cu	0.639	-0.188	-0.078	-0.465	0.927												
Zn	0.407	-0.274	-0.337	-0.378													
Zr	0.178	0.565	0.614														
V	0.198	0.377															
Sr	-0.355																

TABLE 5. Correlation coefficient of elements for Bardawil sediments.

	Ba	Sr	V	Zr	Zn	Cu	Rb	Ga	Y	Pb	Co	Ni	Cr	Nb	Ce	% Clay m.	% Carb. m.
% Detrital m.	0.236	-0.444	0.868	0.605	0.116	0.022	0.106	0.224	0.740	0.576	-0.374	0.269	0.397	0.561	-0.131	0.002	-0.540
% Carbonate m.	0.153	0.871	-0.584	-0.964	-0.633	-0.551	-0.504	-0.752	-0.957	-0.496	0.966	-0.809	-0.850	-0.749	-0.157	-0.838	
% Clay m.	-0.421	-0.796	-0.046	0.778	0.743	0.713	0.546	0.808	0.671	0.665	0.922	0.827	0.804	0.592	0.364		
Ce	-0.991	-0.612	-0.532	0.359	0.775	0.902	-0.670	0.767	0.191	0.930	-0.371	0.707	0.649	0.675			
Nb	-0.612	-0.958	0.256	0.912	0.811	0.846	-0.191	0.906	0.393	0.827	0.930	0.954					
Cr	-0.633	-0.998	0.199	0.940	0.935	0.892	0.575	0.979	0.854	0.866	0.932	0.993					
Ni	-0.701	-0.985	0.091	0.900	0.965	0.933	-0.028	0.995	0.248	0.910	-0.917						
Co	0.383	-0.938	-0.360	-0.959	-0.791	-0.732	-0.367	-0.620	-0.900	-0.685							
Pb	-0.973	-0.838	-0.303	0.644	0.986	0.997	0.366	0.944	0.483								
Y	-0.150	-0.881	0.678	0.978	0.615	0.528	0.335	0.733									
Ga	-0.764	-0.962	0.000	0.856	0.985	0.963	0.099										
Rb	0.641	-0.034	0.566	0.266	0.241	-0.304											
Cu	-0.908	-0.866	-0.259	0.666	0.996												
Zn	-0.862	-0.915	0.155	0.759													
Zr	-0.333	-0.957	0.512														
V	0.595	-0.254															
Sr	0.592																

ter basis for trace element interpretation. The stratigraphic distribution curves given in Fig. 6 show a considerable variation. Generally Jurassic and Cretaceous calcareous sediments exhibit higher values of Ba, Zr and Sr than the other rock units. While the Tertiary and Quaternary sediments are enriched with clay minerals and organic matter (Fig. 6).

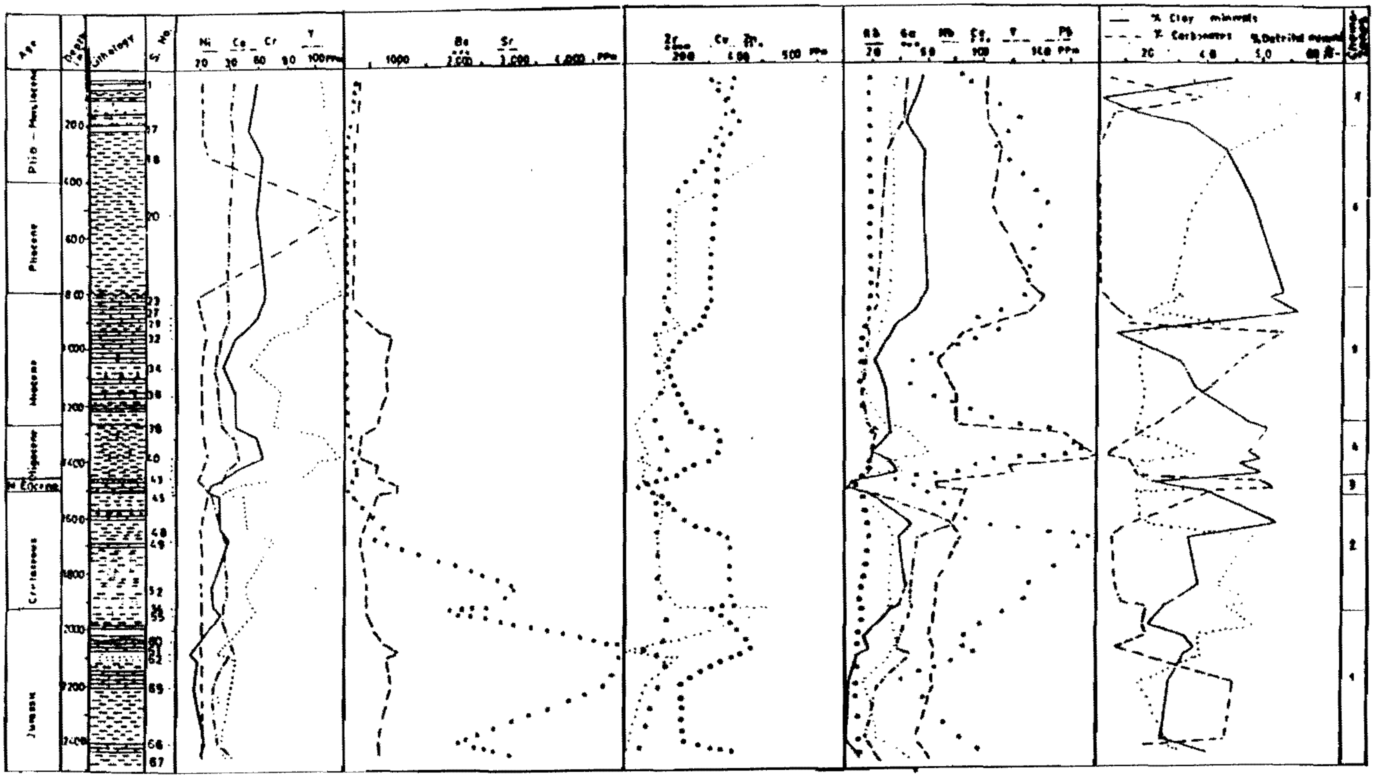

FIG. 6. Stratigraphic variation of trace elements determined in the subsurface sediments of El-Mazar–1 well.

Examination of Tables 3, 4 and 5 indicate positive correlation between organic matter and V, Rb, Cr, Nb and Ce, between V and Ce, Nb, Cr, Y, Ga and Zr and between Zn and Pb and Cu. Moreover, critical study of the vertical distribution shows several important characteristics for the subsurface sequence of El-Mazar–1 (Fig. 6).

1 – Ba increases with increasing in depth. Maximum values are exhibited by Jurassic and Cretaceous sediments (5028 ppm, 4356 ppm), while the Miocene and Pliocene have low values (30 ppm, 94 ppm). The abnormally high values of Ba exhibited by the Mesozoic sediments is related to its precipitation as $BaSO_4$ which occurs as conspicuous concretions in many marine hydrolysate sediments.

2 – The percentage of organic matter decreases with increasing depth (Fig. 7) and exhibits similar variation like clay minerals. A positive correlation was found between organic matter and clay minerals (0.643).

3 – The Pliocene sediments have the highest content of organic matter with an average 8.6% followed by the Miocene 6.5%. Therefore the Pliocene sequence seems to be the most probable source for hydrocarbons.

4 – Zr tends to correlate well with percentage of detrital minerals (0.522). It occurs with a maximum content of about 457 ppm. Its concentration is related to the detrital fraction in silt and sand enriched with feldspar, zircon and mica. Gheith (1982) dealing with the mineralogical and geochemical variations in relation to sedimentation rates in the Hungarian basin found that Ba is always concentrated in the raw material rather than in the separated clay fraction. Furthermore, Gheith and El-Sherbini (1986) reported that Ba and Zr were enriched in sandstone rather than shale. This implies that Ba and Zr are reasonably tied up with the detrital non-clay minerals (feldspar, zircon and mica).

5 – A significant correlation was also found between Sr and percentage of carbonate. It does not follow Ba. Sr^{++} is substituting for Ca^{++} in carbonate minerals.

6 – Ni shows a strong positive correlation with Cr (0.939). Both elements tend to correlate well with Zr, V, Rb and Ga. They are associated with detrital minerals pointing to a continental environment.

7 – The Eocene sediments have relatively low concentration of trace elements and are impoverished in clay minerals. The pH values are of great importance for the sorption of trace elements by clay minerals, Fe and Mn hydroxides, carbonates and organic substances. Förstner (1977) reported low sorption capacity of clay minerals in contact with water having high pH values. Pyrite appears among the mineral components in El-Mazar sediments suggesting changes in the oxidation potential toward high reducing condition corresponding to low values of pH.

8 – The influence of land derived organic matter discharged by the all streams and the nature of the source rocks play an important role for the concentration of trace elements.

9 – V decreases with increasing depth thus rich in the Tertiary sediments and poor in the Mesozoic sediments. The V distribution is similar to that of Cr and Ni and the element has positive correlations with them (0.841 and 0.908). V also exhibits positive correlation with organic matter (0.651) and favours reduced condition of deposition.

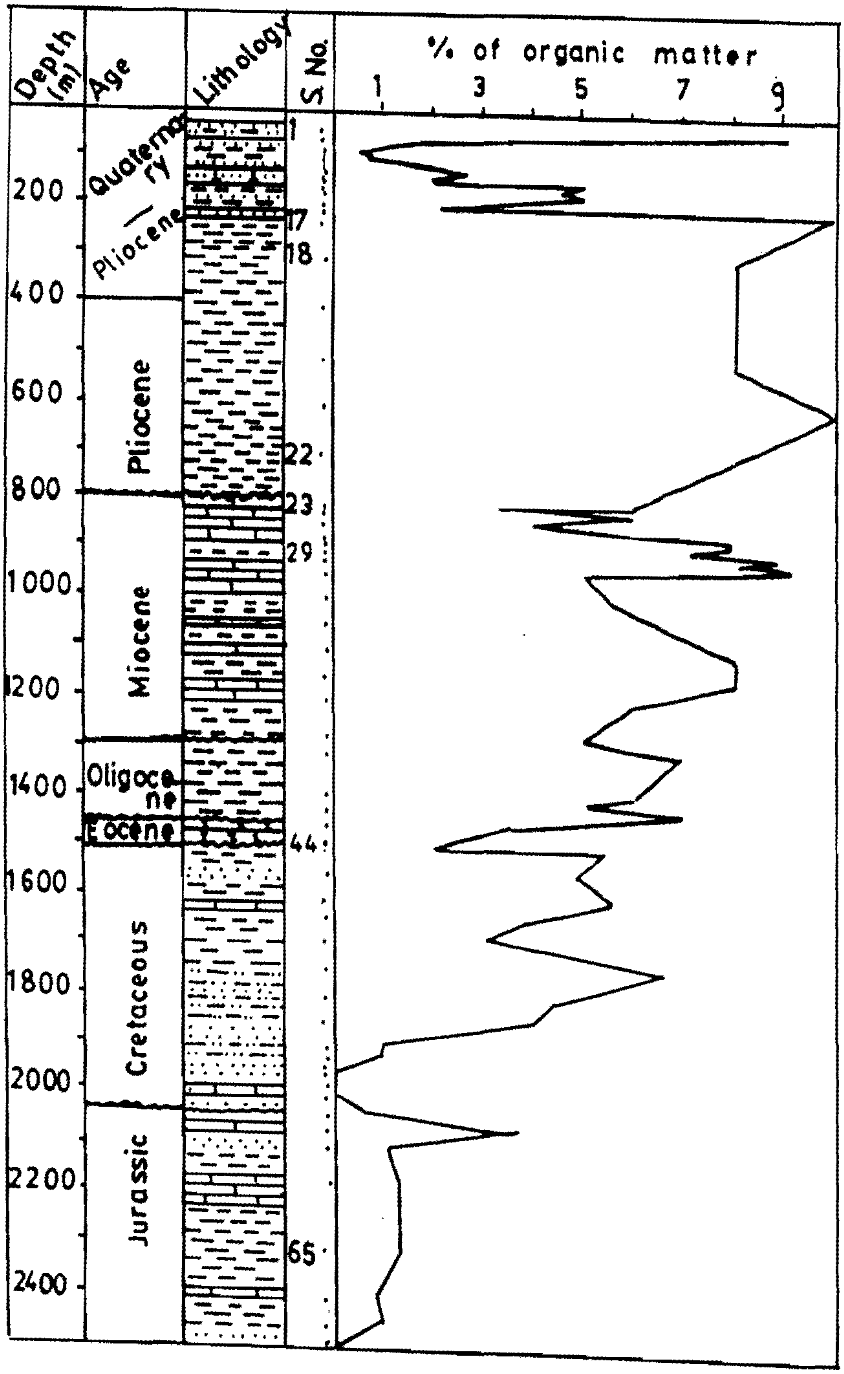

FIG. 7. Stratigraphic variation of organic matter content in the whole rock samples of El-Mazar-1 well.

In conclusion, the abundance variation curves of the trace elements exhibited by the sediments of El-Mazar–1 well and given in Fig. 6 favour their subdivision into seven chemostratigraphic zones (IUGS 1987). The Mesozoic sequence (Jurassic and Cretaceous) shows two zones while the Tertiary sequence distinguished by five zones.

The *1st* chemozone is characterized by high values of Ba and Zr as well as low values of Rb, Ga, V, Pb and Nb relative to the other Mesozoic chemozone. The *2nd* chemozone is distinguished by high values of Zr, Cu and Ce as well as high content of detrital minerals. The *3rd* and *5th* chemozones are characterized by high values of Sr and carbonate minerals as well as low values of V, Zr, Ba, Zn, Cu and Ce. The 4 *th* and *6th* chemozones are distinguished by high values of V, Rb, Cr, Co and Ce. While the upper most chemozone *7th* is distinguished by much more Cu, Cr, V, Zn, and Ce.

The abundance and distribution curves of the trace elements constructed for Malha–1 well (Fig. 8), and the correlation coefficients given in Table 4 emphasize the following criteria :

1 – Ba exhibits a negative correlation with Sr (– 0.355). It has a similar distribution curve to the detrital constituent.

2 – The distribution curves of Ni, V, Zr, Rb and Ga are correlatable well with each other and show similar variation trends to the clay mineral content. They all have a positive correlation (Table 4).

3 – A good correlation was found between Ce and Nb (0.939). Both are correlatable with the clay mineral content (0.617 and 0.708).

4 – Cu and Zn increase with depth. Jurassic sediments have maximum content of Cu (1524 ppm).

5 – The Cretaceous and Jurassic clastics are enriched with trace element due to the high content of clay minerals, suggesting their simultaneous deposition as hydrolysate.

6 – The abundance and variation curves of Malha–1 well favour roughly their subdivision into four successive geochemical units *i.e.* chemozones (IUGS 1987). The *1st* and *3rd* chemozones are distinguished by high values of Cr, V, Ba, Ce, Pb, Cu and Zr. These two chemozones are more argillaceous. The *2nd* and *4th* chemozone are characterized in general by being more calcareous and having low content of the trace elements.

From Bardawil–1 well, four samples only have been analysed for trace element contents. Therefore, conclusions achieved are will not be justifiable.

Conclusions

The samples recovered from the three wells and analyzed for bulk mineral components and trace element contents, their significance and stratigraphic behavior proved the following conclusions :

1 – Kaolinites are dominant in the Jurassic and Cretaceous of El-Mazar–1 well and only in the Cretaceous of Malha–1 well indicating a relative warm climate acting

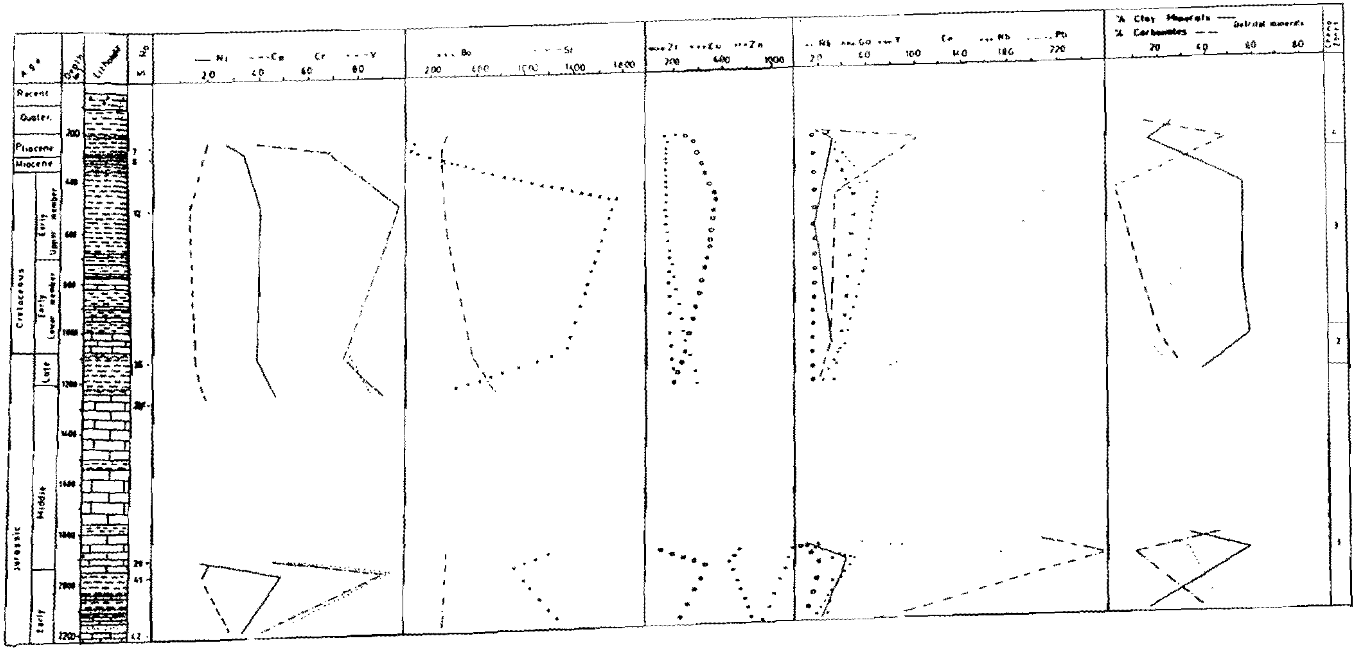

FIG. 8. Stratigraphic variation of trace elements determined in the subsurface sediments of Malha–1 well.

on a terrestrial source with peneplain topography.

2 – Illite is abundant in the Jurassic of Malha–1 reflecting close relation to river-born sediment and tectonically unstable active area.

3 – Montmorillite with subordinate kaolinite are the principal clay mineral components of the Oligocene, Miocene and Pliocene of El-Mazar–1 well.

4 – Montmorillonite is very common in the Miocene and Pliocene of Bardawil–1 well.

5 – The clay minerals (montmorillonite and/or kaolinite) generally constitute the main bulk minerals encountered in the Pliocene of the studied three wells.

6 – Carbonate minerals (calcite dominated over dolomite) are enriched in the Jurassic, Eocene and Miocene of El-Mazar–1.

7 – Arid climate with numerous humid periods are prevailed during the Cretaceous, Miocene and Pliocene of Bardawil–1 and El-Mazar–1 well.

8 – The stratigraphic variations of the geochemical features regarding abundance and vertical distribution of the trace elements revealed high concentration of Ba, Zr, Sr and Pb in the Jurassic and Cretaceous sediments of El-Mazar–1 well.

9 – The Pliocene and Pleistocene sediments are enriched with Co, Cr, Cu, V, Rb and Ce due to the enrichment by terrigenous fine grained materials.

10 – The highest values of organic matter is exhibited by the Pliocene sediments of El-Mazar–1 which seem to be the most probable source for hydrocarbon.

11 – Seven geochemical stratigraphic units (chemozones) are suggested for the subdivision of El-Mazar section, generally correlatable with the lithostratigraphic classification suggested by IEOC.

Acknowledgement

The authors are very grateful to Prof. Dr. Z.M. Zaghloul, Prof. of Geology, El-Mansoura University for his valuable discussion and reading the manuscript. Many thanks are also due to the management of the International Egyptian Oil Company (IEOC) for providing us with the samples studied.

References

Biscaye, B.E. (1965) Mineralogy and sedimentation of Recent Deep Sea clay in the Atlantic Ocean and adjacent seas and ocean.

Carrey, S.W. (1976) *The Expanding Earth: Development in Geotectonics,* 10, Elsevier Publ. Co., Amsterdam, pp. 1-488.

Chamely, H. and **Diester-Haass, L.** (1979) Upper Miocene to Pleistocene climates in north-most Africa deduced from terrigenous components of site 397 sediments (leg 47A DSDP). *Initial reports DSDP,* 47, U.S. Gov. print. off., Washington, DC.1: 641-646.

Chao, G.Y. (1969) *20 (Cu) Table for Common Minerals.* Carelton Univ. Dept. of Geology. Geological paper, 69-2 Ottawa, Canada.

Degense, E.T., **William, E.G.** and **Keith, M.L.** (1958) Environmental studies of Carboniferous sediments. II: Application of geochemical criteria. *Bull. Amer. Assoc. Petrol. Geol.* **42:** 981-997.

El-Gindy, A.R. and **Samuel, M.D.** (1978) Major changes in the clay mineralogy of Egyptian Phanerozoic mudrocks and marls. *Iraq J. Geology 5th Conf.* 1-53.

Förstner, U. (1977) Metal concentrations in recent lacustrine sediments. *Stütgart Arch. Hydrobiol.* **80:**(2): 172-191.

Gheith, A.M. (1982) Mineralogical and geological variations in relation to sedimentation rates in the Hungarian basin. *Acta Geologica Academiae Scientiarum Hungaricae,* **25:** 365-393.

Gheith, A.M. and **El-Sherbini, M.I.** (1986) On the Mineralogy and Geochemistry of subsurface sediments in the northern part of the Nile Delta, *Egypt. J. Geol.* **30,** (1-2): 9-24.

Gheith, A.M., El-Sherbini, M.I. and **Hassab-Allah, R.R.** (1993) Scenario of sedimentation in relation to tectonic along Bardawil lake, coastal margin of Northern Sinai, Egypt. *J. KAU: Marine Science,* **4:** 55-71.

Hirst, D.M. (1962) The geochemistry of modern sediments from the Gulf of Paria–II. The location and distribution of trace elements. *Geochim. Cosm. Acta.* **26:** 1147-1187.

IUGS International Union of Geological Science and the Committees of Quantitative Stratigraphy (1987) *Quantitative Stratigraphy: Episode,* **10,** No. 2, p. 14.

Krauskopf, K.B. (1956) Factors controlling the concentration of thirteen rare metal in sea water. *Geochim. Cosm. Acta* **9:** 1-32.

Livermore, R.A. and **Smith, A.G.** (1985) Some Boundary Condition for the Evolution of the Mediterannean Region: *In:* **Stanley** and **Wezel** (ed.), *Geological Evolution of the Mediterranean Basin,* Springer-Verlag, pp. 323-346.

Pei-Yuan, Chen (1977) Table of key lines in X-ray powder diffraction patterns of minerals in clays and associated rocks. *Dept. of Natural Resources, Geol. Survey Occasional paper,* 21.

Singer, A. (1984) The Paleoclimatic interpretation of clay minerals in sediments, a review. *Earth Science Reviews,* **21:** 251-293.

معدنية وجيوكيميائية رواسب المتوسط - الثلاثي تحت السطحية عند بحيرة البردويل ، شمال سيناء بمصر

أمين غيث* ، محمود الشربيني و رجب حسب الله

*قسم الجيولوجيا البحرية ، كلية علوم البحار بجامعة الملك عبد العزيز ، جدة ، المملكة العربية السعودية و قسم الجيولوجيا ، كلية العلوم ، جامعة المنصورة ، جمهورية مصر العربية

المستخلص . يعالج هذا البحث التركيب المعدني والجيوكيميائي للرواسب تحت السطحية في ثلاثة آبار عميقة حفرت في منطقة بحيرة البردويل وهي : (مالحة - المازار - والبردويل) بشمال سيناء .

ولقد تم تعيين التركيب المعدني الكلي في ٥١ عينة أصلية من الغرين والحجر الجيري بواسطة الأشعة السينية ، حيث وجد أن معدن الكاولينيت سائد في رواسب عصري الجوراسي والطباشيري في بئر المازار ، وأيضًا رواسب الطباشيري في بئر مالحة مما يعكس بيئة ترسيب تمتاز بمناخ دافيء وانخفاض في مستوى سطح البحر .

بينما وجد معدن الاليت سائد في رواسب الجوراسي في بئر مالحة مما يعكس أهمية موقع بئر مالحة من حيث إنها مساحة نشطة غير مستقرة تكتونيًا .

أما رواسب الاوليجوسين ، والميوسين والبليوسين فتمتاز بكثرة معادن المونتموريللونيت ، الكاولينيت ، الكلوريت والاليت في ترتيب تناقصي في السيادة مما يدل على مناخ رطب .

كما حللت هذه العينات بواسطة أشعة الفلورسنت لمعرفة محتواها من العناصر النادرة حيث لوحظ أن التوزيع الطبقي لعناصر الباريوم ، الزيركونيوم ، الاسترانشيوم والرصاص تعكس تركيز عالي في رواسب الجوراسي والطباشيري لبئر المازار بينما تتركز عناصر الكوبلت ، الكروم ، الفانديوم ، النحاس ، الرصاص في رواسب البليوسين والبليستوسين ، ولقد أمكن تقسيم القطاع الرسوبي تحت السطحي لبئر المازار إلى سبعة نطق جيوكيميائية تتطابق مع التقسيمات الليثواستراتيجرافية المقترحة .